ADVANCED FUNCTIONAL MATERIALS
www.afm-journal.de

Facile Fabrication of Ordered Crystalline-Semiconductor Microstructures on Compliant Substrates

Francesca Cavallo, Kevin T. Turner, and Max G. Lagally*

Buckling and wrinkling of thin films on a compliant material has proved to be a resource in several applications, such as flexible electronics, thin-film metrology and fabrication of tunable optical components. A versatile approach for the fabrication of two-dimensional and linear arrays of buckled structures is demonstrated here using a stiff material, in the form of a nanomembrane, on a compliant substrate. The novelty of the fabrication process is that the substrates are strained by isotropic volume expansion in solvents. This work illustrates in detail the potential of our technology to fabricate ordered arrays of 3D structures on large-area compliant substrates, with important implications for a large number of fields. Furthermore, this paper discusses the interesting interface chemistry and mechanics leading to controllable and reproducible fabrication of our 3D structures.

1. Introduction

The buckling of thin films of inorganic, inherently stiff materials (e.g., group IV and III-V semiconductors, various metals and insulators) on compliant substrates via localized delamination has recently proved to be a resource in flexible electronics and optoelectronics.[1–4] As a result, efforts have been initiated to understand and control buckling instabilities of such films supported by and bonded to compliant materials.[1–8] Combining thin sheets of inherently stiff materials in a wavy or buckled geometry with compliant substrates has value beyond just flexible electronics, however. For example, one can manipulate stiff-thin-film buckling to create arrays of three-dimensional features of specified height or length or spacing, or combinations of regions without delamination and with controlled delamination. Depending on the nature of the material, such structures have potentially many applications in biotechnology,[9] in microfluidics,[10] in photonics,[11] and in hybrid fields such as optomechanics[12] and optofluidics.[13] Additionally one would like to understand the physics, chemistry, and mechanics that lead to controlled and repeatable fabrication of such structures, so that one can create predictive strain engineering methods for combining a large variety of hard and soft materials.

In this work we describe a facile and versatile approach for the fabrication of two-dimensional and linear arrays of buckled structures using a stiff material, in the form of a very thin sheet, on a compliant substrate. Our method is based on a guided self-assembly procedure that combines top-down patterning with self-organized stress relaxation. We demonstrate the approach with thin sheets of single-crystalline silicon on polydimethylsiloxane (PDMS), but the procedure is general and can therefore be applied to different combinations of stiff films/compliant substrates.

Dr. F. Cavallo, Prof. K. T. Turner,[+] Prof. M. G. Lagally
University of Wisconsin-Madison
WI, 53706, USA
E-mail: fcavallo@wisc.edu
[+]Present address: University of Pennsylvania, Philadelphia, PA 19104-6315, USA

DOI: 10.1002/adfm.201303165

2. Results and Discussion

Our approach to obtain 2D-arrays of buckle-delaminated structures is outlined in **Figure 1**a–d. We start in all cases with silicon-on-insulator (SOI) wafers, in which a thin top template layer of Si is supported by a SiO_2 buffer layer on a Si handle substrate. These thin Si templates are patterned, while on their original SiO_2/handle Si substrates, in a near checker-board fashion with rectangular regions (referred to as NM islands) connected only at their corners by narrow strips, Figure 1a. After release, via etching of the buried oxide in HF, the Si template layer, now referred to as a silicon nanomembrane (SiNM),[14–16] is transferred (Figure 1b) to a thick PDMS substrate whose surface is oxygen plasma treated. The transfer of the SiNM to the new host is performed using a wet or dry technique, as detailed in the Experimental Section. Exposure to an oxygen plasma makes the PDMS surface hydrophilic by introducing silanol groups (Si–OH) at the expense of methyl groups (Si–CH_3).[17,18] We transferred NMs to both hydrophobic and hydrophilic PDMS substrates and found that OH-termination allows more reliable transfer of large-area membranes in a planar geometry.

The NM/PDMS combination is subsequently immersed in a solvent, Figure 1c. Isotropic volume expansion is induced in the elastomer when it swells in a solvent.[17] As detailed later in the text, we observe that a negligible amount of strain is transferred to the NM during this step. After treatment in solvent the NM/PDMS is exposed to air at room temperature, resulting in evaporation of the solvent and contraction of the substrate to its original dimensions, Figure 1d. During this step, the SiNM bonds to the PDMS substrate and compressive stress, σ, is applied to it. Specifically a higher stress is applied at the interconnect strips due to their reduced width compared to the NM islands, resulting in delamination and out-of-plane buckling at the interconnects only. We do not observe any global or localized buckling mode superimposed on the buckling at the

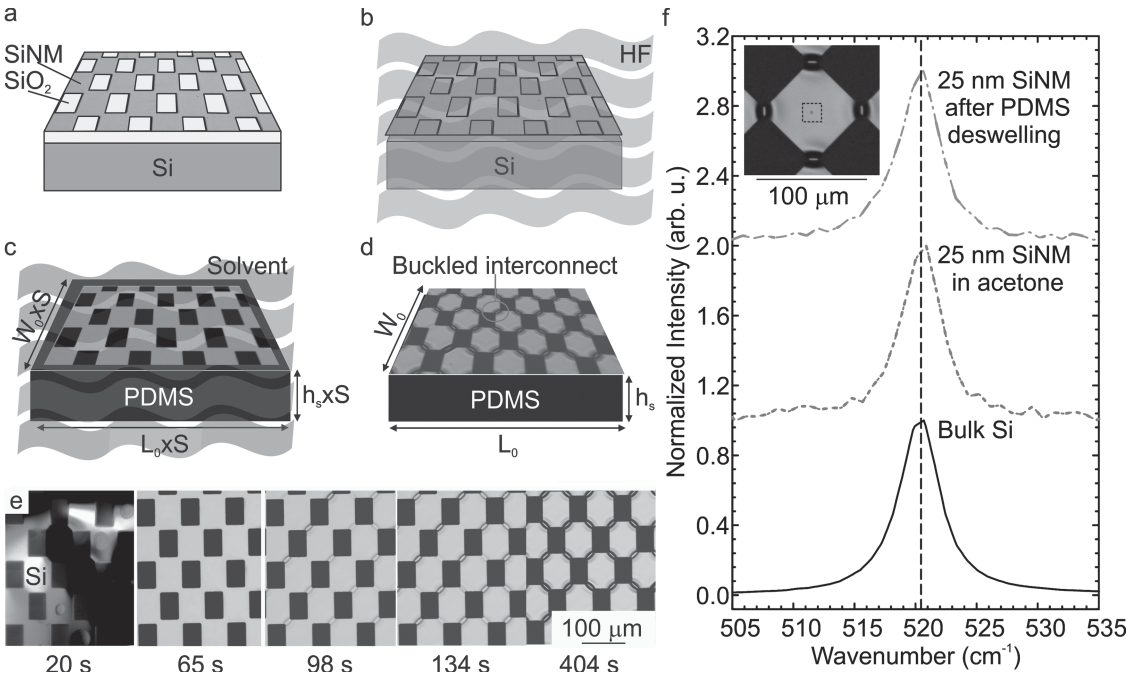

Figure 1. Schematic illustration of the procedure used to obtain 2D-arrays of ordered buckle-delaminated structures, and evolution of buckling instability. a) The SiNM on its original SiO_2/handle Si substrate is patterned into a near checker-board geometry by optical lithography and reactive ion etching. b) The SiNM is released from the original substrate by selective etching of the buried SiO_2 in HF. c) The SiNMs is transferred to the PDMS substrate and the combination is immersed in solvent. Treatment of the NM/PDMS in solvent results in isotropic volume expansion of the PDMS by a factor S, i.e., the swelling ratio of the substrate in the solvent. SiNMs are unstrained during this step. d) SiNM/PDMS after exposure to air, leading to deswelling of the PDMS substrate. The compressive strain transferred to the NM during this step induces buckling-delamination at the interconnect regions of the film. e) Selected video frames showing the evolution of buckling instability during deswelling of the substrate for a 25 nm SiNM on PDMS treated in acetone for 30 min and rinsed in isopropyl alcohol (IPA) for 120 s. The NM is patterned in a 2D array of interconnected islands with a total lateral dimension of 4 mm × 6 mm. Only a portion of the NM is visible in the images. At 20 s solvent is present on the sample surface. At progressively longer times the NM bonds to the PDMS surface and forms into buckle-delaminated structures at the interconnect regions. f) Raman spectra obtained from a 25 nm SiNM/PDMS combination while in the solvent, ≈2 h after it was submerged (red dotted line) and after exposure to air for 30 min, resulting in deswelling of the PDMS to its original dimensions (green dash-dotted line). Measurements were performed by focusing the excitation laser approximately in the center of the NM islands. The inset is an optical micrograph of the NM (in light yellow) after buckling has occurred at the interconnects. The size of the laser spot and therefore the area probed are indicated by the red circle highlighted by a box. A Raman spectrum obtained from bulk Si (black solid line) is also shown for comparison.

interconnects as long as we have patterned the substrate with a periodic array of such stress concentrators.

Buckling-delamination at the interconnect regions during solvent evaporation is illustrated with selected chronological video frames in Figure 1e, starting ≈20 s after the sample was removed from the solvent. A 25 nm-thick SiNM patterned in a 2D array of interconnected NM islands transferred to PDMS had been immersed in acetone for 30 minutes, then rinsed in isopropyl alcohol (IPA) for 120 s and left in air. At 20 s in air, solvent droplets are still visible on the surface of the NM. Frames taken at 65 s show no trace of solvent on the surface, and the array of interconnected areas lying flat on the substrate surface. Buckling-delamination of the interconnect regions, and only these regions, occurs between 65 s and 134 s of sample exposure to air. From 134 s to 404 s the buckles increase in height, as indicated by the higher contrast compared to the planar NM islands.

We performed Raman spectroscopy of the NM/PDMS while in solvent in order to investigate the extent of deformation of the NM while swelling of the substrate occurs. For this purpose we focused a 633 nm wavelength excitation laser to a ≈2 μm spot (see Experimental Section for details). We probed the NM in the center of the large regions between the interconnects, as shown in the inset in Figure 1f. Raman spectra were acquired from a 25 nm SiNM/PDMS sample ≈2 h after the specimen was first submerged in acetone. The spectrum in Figure 1f is dominated by a peak centered at 520.4 cm^{-1} corresponding to the first-order longitudinal optical phonon of the Si-Si mode in unstrained Si[19] (see bulk-Si spectrum in Figure 1f). This result confirms that the NM stays undeformed while PDMS swells in solvent. We explain this behavior by using a stick-slip model, as follows: we expect the adhesion between the NM and PDMS to be mediated by van der Waals interactions between H on the NM surface and OH groups on the plasma treated PDMS. Indeed extensive investigations of the surface of bulk Si after treatment in HF have been conducted in the past decades, revealing that the Si surface is primarily terminated by hydrogen, with some fluorine also detected.[20–22] As-released NMs have an identical surface termination as bulk Si treated in HF.[23] Once the NM/PDMS is immersed in solvent, the PMDS starts swelling. The NM stretches along with the PDMS in this phase. However, because the NM is weakly bonded to

the PDMS, at a certain critical degree of swelling of the PDMS the shear stress applied at NM/PDMS interface is high enough to generate an interface crack.[24–26] As a result the NM (to the extent that it was strained tensilely at all) relaxes towards its unstretched state through slipping at the interface with the PDMS. At this point we expect the two materials to re-bond by van der Waals forces and the stick-slip process to repeat as swelling progresses further and an increasing shear load is applied to the interface. To summarize, the NM undergoes oscillations between sticking and slipping on the PDMS until the substrate reaches its equilibrium dimensions in the solvent, which results in no stretching of the NM during swelling.

Raman measurements were repeated after the NM/PDMS was exposed to air for 30 min, that is, a sufficient time for the acetone to evaporate and the PDMS substrate to shrink back to its original size. Figure 1f shows a typical Raman spectrum acquired from the NM islands after the last process step. Comparison with the spectrum acquired from unstrained bulk Si shows that a negligible amount of strain is transferred to the large NM islands also during deswelling. We ascribe this result to the relatively high stiffness of the NM compared to the PDMS, as detailed below. Again, we expect that a bond forms between the NM and the PDMS as solvent evaporates. The deswelling strain has to be accommodated through deformation of both the NM and the PDMS. The deswelling should lead to the PDMS applying some compressive strain on the large Si regions. However, the amount of strain transferred to the NM in the large islands depends on the relative stiffnesses of the Si NM and the PDMS substrate according to a simple strain-sharing model.[27] A resonable assumption in our argument is that the NM deforms axially during deswelling, due to its nanoscale thickness. On the other hand the PDMS substrates in our experiments have a 3 mm thickness, which is significantly larger than the NM thickness and lateral dimensions of the NM islands. As a result the PDMS effectively acts as an elastic half-space[28] and the deswelling strain is accomodated through shear deformation of the elastomer. We calculated the axial and the contact shear stiffness[28] of a 25 nm SiNM and a 3 mm PDMS on a 60 μm × 60 μm area, corresponding to the size of the NM islands in the inset in Figure 1f. We obtained values of ≈3200 N m^{-1} and ≈3 N m^{-1} for the SiNM and PDMS substrate, respectively. This shows that in the large islands the NM is effectively much stiffer than the PDMS and, thus, almost all of the strain is accommodated in the PDMS. We would then expect the PDMS to be relaxed in the areas where delamination took place, and highly tensilely strained in the regions beneath the bonded Si NM, but we have not been able to confirm that.

We are able to demonstrate the scalability with NM thickness of the out-of-plane dimensions (i.e., amplitude vs length) of buckle-delaminated structures arranged in a 2D array. The sketch in **Figure 2**a shows top and three-dimensional views of a single buckle-delaminated structure. Optical lithography was used to define rectangular NM regions connected by strips of various widths. Stress concentration at these regions leads to buckles with widths in a range of ≈5 to ≈30 μm. Figure 2b shows top-view optical images of NMs with delaminated stress concentrator regions (buckles) arranged in a periodic fashion on a PDMS substrate. Figure 2c is a tilted SEM image of an array of buckled regions formed, after solvent evaporation, in

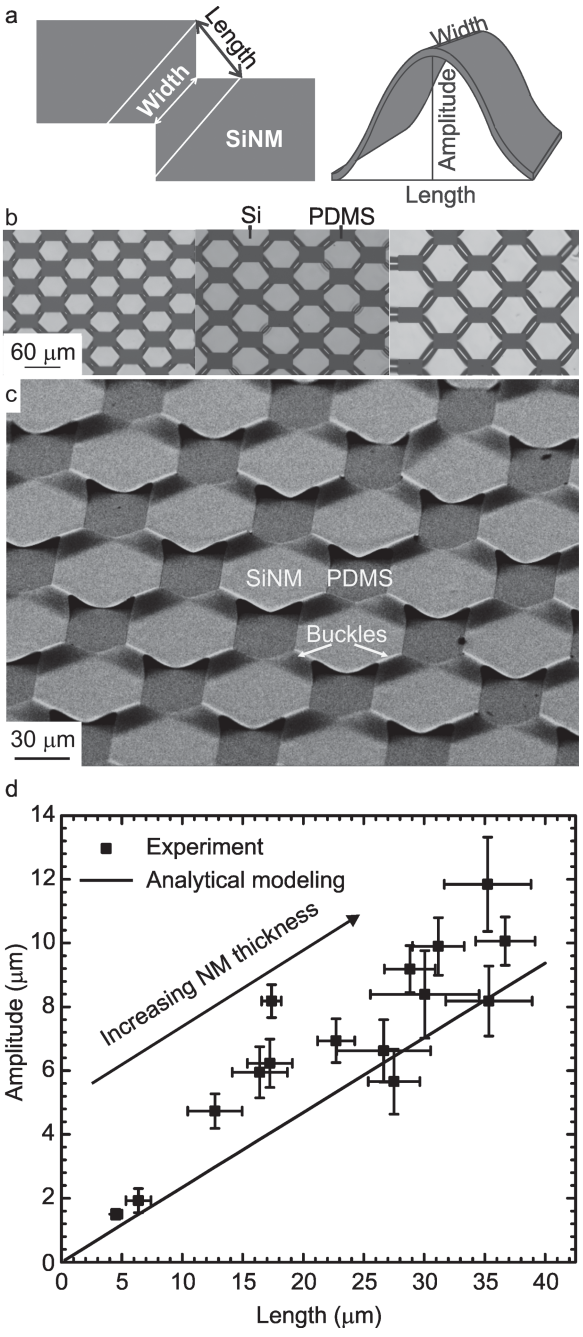

Figure 2. Structure and scalability of buckle-delaminated regions arranged in 2D-arrays. a) Schematic diagrams illustrating (left) a top view of the SiNM in proximity of the interconnects, where delamination occurs; (right) a 3D view of a buckle-delaminated structure. On the left the delaminated portion of the NM is included between two continuous lines. b) Top-view optical images of 2D arrays of ordered buckle-delaminated regions formed by a 72 nm SiNM/PDMS system immersed in acetone for 2h. From left to right buckles of different widths are shown. c) Tilted SEM image showing a 72 nm SiNM formed into delaminated buckles at the interconnects of the near-checkerboard pattern. d) Amplitude vs length for buckled NMs of various thicknesses in the range of 17 to 270 nm. NMs of all thicknesses were patterned as shown in in Figure 1a prior to transfer to the PDMS substrate. Each data point in the plot corresponds to a different NM thickness in the range specified above. The data are compared to calculated results using energy minimization.

a 72 nm-thick SiNM on PDMS immersed in acetone for 2 h and rinsed in isopropyl alcohol (IPA) for 120 s. These conditions correspond to a maximum possible solvent-induced strain of $\varepsilon \approx 11\%$. The calculation of the applied strain for a given solvent treatment is described in the Experimental Section. SEM images confirm that the NM stays flat away from the stress concentration regions and that no coherent deformation of the PDMS substrate occurs during buckling. Figure 2d demonstrates the scalability of the out-of-plane dimension of the buckled structures with NM thickness, at a given applied strain $\varepsilon \approx 11\%$. We point out that only the NM thickness is varied in a controlled fashion in this study. At each NM thickness a buckled structure with a different length-amplitude combination is obtained through self-assembly of the NM under compression. Specifically amplitude and length are defined concomitantly by a number of parameters including the thickness and elastic properties of the NM and substrates, the applied strain during deswelling, the boundary conditions, and the interface toughness. Buckle-delaminated structures with amplitudes varying between 1.6 and 14 μm at corresponding lengths in a range of 2 to ≈40 μm are obtained from NMs with thicknesses between 17 and 270 nm. We compare these experiments with results obtained from analytical modeling using energy minimization, following the analysis of Song et al.[18] The buckle amplitude values are underestimated by 15–20% using the analytical model. We attribute this discrepancy to the use of a fixed boundary condition for the NM (i.e., clamped NM at the edge of the delamination) in the calculation of the strain energy (see Figure S1, Supporting Information).[8]

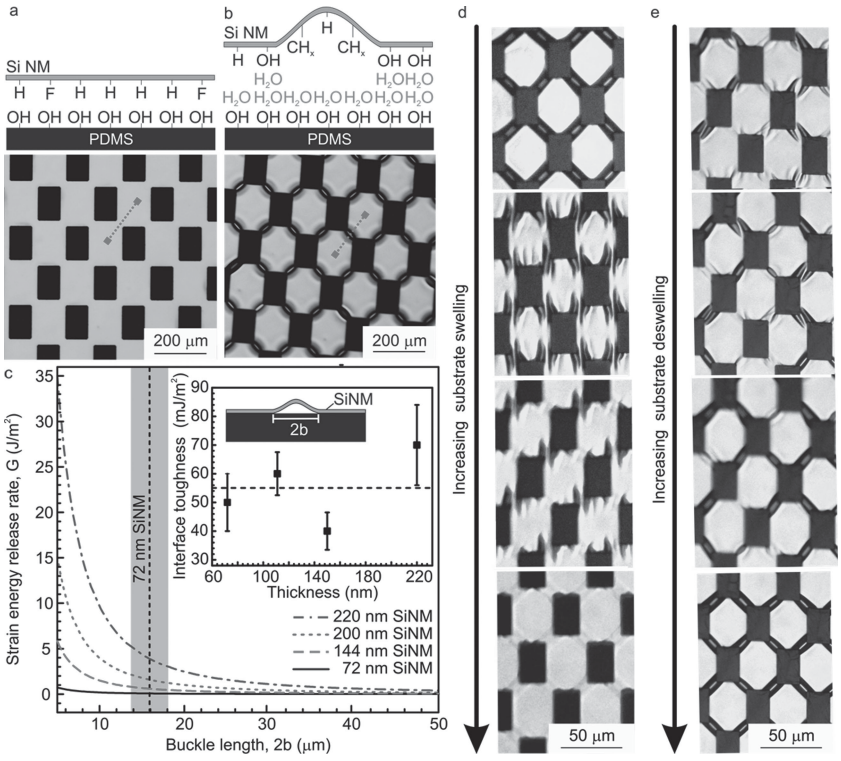

Figure 3. Interface adhesion mechanisms during fabrication of the 2D array of buckle-delaminated structures, and after a buckling instability has occurred. SiNMs are transferred to an oxygen plasma treated PDMS substrate immediately after release from their original handling substrate. The SiNM/PDMS combination is placed in acetone for 3 h, followed by a rinse in IPA for 120 s. a,b) Schematic cross-sectional views and top-view optical images of a 25 nm SiNM/PDMS system a) before and b) upon treatment in solvent and deswelling. The schematic drawings show the termination of the Si and PDMS surfaces at the two stages of the fabrication process and along the direction indicated by the dashed lines in the optical images. c) Calculated values of strain energy release rate vs buckle length for SiNMs of various thicknesses. The dashed vertical line and the area shaded in gray correspond to the average buckle length and standard deviation measured over 20 buckled structures formed by a 72 nm SiNM/PDMS. Corresponding values of the strain energy release rate G are obtained from the intercept with the black solid line. The inset summarizes the values of interface toughness, obtained for all investigated NMs. The average of the values, 55 mJ m^{-2}, suggests that adhesion between the NM and the host substrate is primarily mediated by van der Waals interactions. d) Selected video frames showing a 72 nm SiNM on PDMS (buckled at the interconnects) while the substrate undergoes reswelling in acetone. After 2 h in solvent the buckled structures have disappeared. However, the contrast at the interconnects suggests that the NM does not bond back on the substrate surface. We attribute this behaviour to liquid trapped at the NM-PDMS interface at the interconnect regions. e) Buckled structures increase in height at the interconnects when the sample shown in (d) is again exposed to air to cause deswelling.

The nature of the interface bond between the NM and PDMS at various stages of the process is crucial to the formation as well as to the stability of our fabricated structures. Stability will be a requirement in potential applications of buckled structures to confine/guide particles or biological cells or as channels for microfluidics. The NM/PDMS bond in the unbuckled regions must be liquid-tight and strong enough to withstand pressure-driven liquid flow.[24–26] Yet our approach to achieve ordered arrays of buckled structures must rely on a relatively weak bond between the SiNM and the PDMS substrate during immersion in solvent (see Figure S2, Supporting Information). In the following we discuss the nature of the interface bond between the NM and the PDMS substrate as well as its evolution. Specifically we present experimental results and fracture mechanics calculations suggesting that: 1) weak interactions are responsible for the adhesion between the NM and the PDMS while the interface is enveloped in solvent and upon solvent evaporation, but 2) a strong bond forms between the NM and the PDMS after a longer exposure to air. These conclusions are limited to the unbuckled NM/PDMS areas and they are supported by **Figure 3**. Figure 3a,b shows schematic cross-sectional views along with top-view optical images of a 25 nm SiNM on PDMS before immersion in solvent (Figure 3a) and upon solvent evaporation (Figure 3b). The schematic diagrams illustrate possible surface terminations of the NM and the PDMS along the directions specified by the dashed lines in the optical images. We already discussed the nature of the surface termination of the NM and PDMS before the NM is transferred to the elastomer. Figure 3b schematically illustrates the PDMS and Si surface

terminations upon treatment in solvent resulting in water molecules adsorbed on both the NM and the PDMS surfaces in proximity of OH groups. (The nature of Si and PDMS surface termination upon solvent evaporation is discussed in more details in the Supporting Information.) As a result the adhesion between the SiNM islands and the PDMS upon delamination at the interconnects may be mediated by: 1) hydrogen bonds between water molecules at the interface, and 2) weak van der Waals interactions between OH groups on the PDMS surface and the localized CH_x-based groups on the SiNM surface (see Figure 3b).

We are able to quantify the interface toughness, that is, the resistance to interfacial debonding,[29] of the NM-PDMS bond by relating the measured lengths of the debuckled NM regions to the strain energy release rate of the system, by using the Griffith energy-balance approach.[29] The buckled NM is treated as a crack, with the line separating the bonded and unbonded portions of the film as the crack front. For the structures in our experiment, the governing equation for Griffith-based fracture mechanics is:

$$-\frac{\mathrm{d}\Delta U}{\mathrm{d}A} = \Gamma \tag{1}$$

where ΔU is the strain energy stored in the buckled NM (i.e., the difference in the strain energy of the NM in the unbuckled and the buckled states), Γ is the sum of the surface energies of the unbonded Si and PDMS surfaces (minus the interface energy), and A is the delaminated (i.e., unbonded) area of NM. The left-hand side of the expression is known as the strain energy release rate (G), and the right-hand side of the expression is typically taken to be the interface toughness. We calculate G at varying buckled length, $2b$, for NMs of four different thicknesses, using the approach described by Yu and Hutchinson.[30] (The model reported in the literature[30] was modified as specified in the Supporting Information.) The results are plotted in Figure 3c. Thus, by measuring the length of the buckled portion of the NM (see Experimental Section), we can directly determine G and the interface toughness between the Si and PDMS surfaces (see Equation 1). In Figure 3c the dashed line and the area shaded in gray correspond to the average buckle length and standard deviation measured over 20 buckle-delaminated structures formed by a 72 nm SiNM/PDMS structure. A range of corresponding values of interface toughness is determined by the intercept of the area shaded in gray and the black solid line, i.e., the calculated strain energy release rate for a 72 nm SiNM/PDMS sample. The same procedure is applied to all NM thicknesses we have investigated. The inferred values of interface toughness range between 32 and 84 mJ m^{-2} (see the inset in Figure 3c), somewhat higher than the values measured for van der Waals bonds (20–30 mJ m^{-2}).[22] This result confirms that a mechanism in addition to the van der Waals interactions is responsible for the adhesion between the NM and the PDMS in the unbuckled areas. As suggested previously, hydrogen bonds may form in localized areas between water molecules absorbed by the two surfaces during solvent evaporation.[22]

Finally, we test the strength of the NM/PDMS bond (in the unbuckled areas) in liquid and under applied stress by re-swelling in solvent samples where buckling had previously occurred. Tests are performed 45 min, 48 h, and 100 h (we call these times the bonding times) after the buckling instability of the NM is first observed. For this purpose, we investigate the mechanical response of a 72 nm NM/PDMS system patterned in a checker-board fashion and buckled at the interconnects, that is re-immersed in acetone for 2 h. Figures 3d-e show selected video frames of a NM/PDMS with 100 h bonding time, while it is in the solvent. The NM stretches along with the substrate, resulting in a decrease of the out-of-plane dimension of the buckled structures (see Figure 3d). When the sample is again exposed to air at room temperature, buckles at the interconnects rise back to their original amplitude and length (see Figure 3e). The same behavior obtains for the sample with a 48-h bonding time, but not for the 45-min bonding-time sample. This experiment shows that an irreversible seal has formed between the NM and the PDMS in the unbuckled areas somewhere between 1 and 48 h after buckled structures have formed. We suggest the bonding strength increases as water molecules residing between the NM and PDMS slowly diffuse out of the interface. Some opposing OH groups may then be close enough to form a covalent bond across the interface, leading to an overall increase in the energy required to initiate the interface crack formation.[22]

A different perspective can be obtained with linear arrays of buckled channels. For this purpose the silicon templates are patterned into strips with a width of 20–100 μm and length of 1 cm before undergoing the process outlined in Figure 1b–d (see Figure S3 in Supporting Information). In this configuration, two types of instability, namely wrinkling and buckling-delamination,[7,8] are observed for relatively thin and thick NMs, respectively. The two deformation modes are schematically illustrated in **Figure 4**a,b. Wrinkling involves no delamination, but rather coherent deformation of the substrate along with the film, whereas buckling-delamination describes films partly detached from the substrate. Minimization of the elastic strain energy under the constraints applied to the system determines the deformation mode that occurs in the NM.[8] For a thin elastic film bonded to a thick elastic substrate, the instability is constrained by the substrate. The deformation mode (i.e., wrinkling or buckling-delamination) that is favored at the onset of instability depends on the elastic mismatch between the film and the substrate as well as on the size of any pre-existing interfacial delamination between the NM and the substrate.[7,8,30] A detailed discussion of the selection rule between wrinkling and buckling-delamination for the materials used here is reported in the Supporting Information.

Top-view optical and corresponding off-normal SEM images of 55 and 220 nm SiNMs/PDMS immersed in acetone for 20 h are shown in Figure 4a,b, respectively. Scanning electron microscopy of a 55 nm film clearly shows a close-to-coherent deformation of the substrate along with the film (see Figure 4a). On the other hand 220 nm thick SiNMs on PDMS, immersed in acetone also for 20 h, exhibit buckling-delamination (see Figure 4b). For both 55 nm and 220 nm SiNMs a periodic arrangement of the 3D structures is obtained.

We are able to demonstrate the scaling, with NM thickness and with strain, of the out-of-plane dimensions (i.e., amplitude vs length) of linearly arranged wrinkled/buckle-delaminated structures. To investigate scaling of buckle dimensions with thickness we use Si nanoribbons (SiNRs) with a 20 μm width

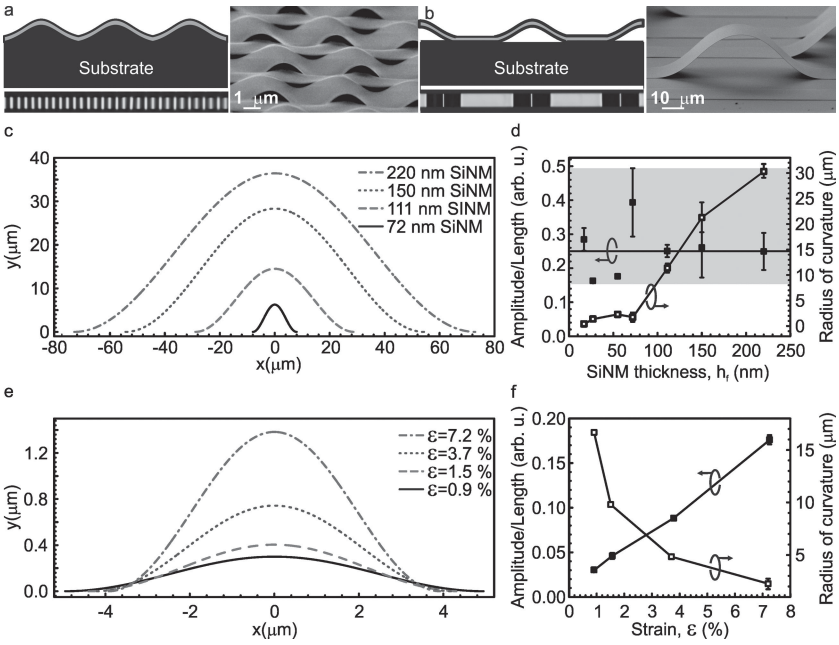

Figure 4. Linear arrays of wrinkled or buckle-delaminated structures for various NM thicknesses and applied strain. a,b) Schematic illustration, optical images, and corresponding off-axis SEM images of a 55 nm SiNM formed into wrinkles (a) and a 220 nm SiNM formed into buckle-delaminated structures (b). In the wrinkled structure the substrate also deforms periodically. The lateral dimensions of the strips are the same for both. For both samples the instability results from treatment to swell the PDMS in acetone for 20 h and exposure to air for 10 minutes to deswell the PDMS. c) Buckle-delaminated NM profiles for different NM thicknesses plotted, with *A* and *2b* corresponding to measured amplitude and length of the buckled structures. d) Maximum-amplitude/length ratio and radius of curvature at the amplitude maximum of wrinkled and buckle-delaminated structures as a function of NM thickness. Data plotted for a NM thickness lower/higher than 60 nm correspond to wrinkles/buckle-delaminated structures. Over the range of thicknesses used, the average ratio of maximum-amplitude/length is 0.25 (black solid line).The area shaded in gray shows the range of values. The radius of curvature at the amplitude maximum increases from 0.3 to 30 μm as the SiNM thickness increases to 220 nm. For all samples in (c,d) conditions are identical: immersion in acetone for 20 h, rinse in IPA for 120 s, and exposure to air for 10 min. e) Wrinkles profiles of a 55 nm SiNM for increasing applied strain, plotted as in (c). The 55 nm SiNM/PDMS structures were immersed in different solvents for 20 h and exposed to air for 10 minutes before characterization. The different solvents produce applied strains ε in the range of 0.9 to 7.2%. (f) Ratio of maximum-amplitude/length and radius of curvature at the amplitude maximum, as a function of strain, for the curves shown in (e).

and thickness $h_f = \{17, 27, 55, 111, 150, 220\}$ nm. After release and transfer to PDMS, all SiNRs are immersed in acetone for 20 h, corresponding to an applied strain $\varepsilon = 7.2\%$. (The maximum swelling is obtained already after ≈1 h, the much longer time is chosen to assure a steady state in the bonding). Wrinkling occurs for $h_f < 60$ nm, and buckling-delamination for NRs of greater thicknesses. Both wrinkled and buckle-delaminated structures are nearly sinusoidal. In Figure 4c the out-of-plane displacement of buckle-delaminated SiNRs is plotted as $y(x) = \frac{A}{2}\left[1 + \cos\left(\frac{2\pi x}{2b}\right)\right]$, with y and x specifying the out-of-plane and in-plane displacement of the NM, respectively, and A and $2b$ corresponding to amplitude and length of the delaminated structures measured as described in the Experimental Section. Both the maximum amplitude and length of the delaminated structures increase with thickness, while the maximum-amplitude/length ratio varies around an average value of 0.25 (see Figure 4c,d). This result indicates that channels or scaffolds of various cross-sectional areas can be fabricated using NRs of various thicknesses, with significant implications for applications in microfluidics and biology. In a different application sphere one might take advantage of deformation instabilities to strain-engineer thin films and change their electronic properties locally.[31,32] Specifically one might fabricate wrinkled and buckle-delaminated structures with various radii of curvature to tune the degree of lattice distortion in the buckled regions of the NM. Figure 4d shows that the radius of curvature at maximum amplitude increases with NM thickness for both wrinkled and buckle-delaminated structures, with the range of values obtained using buckling-delamination (i.e., ≈2–30 μm) being much larger than the one measured for wrinkles (i.e., ≈0.3–2.4 μm). Simple geometrical considerations allow estimation of the strain on the top surface of a deformed NM (wrinkled or buckle-delaminated) if one knows the radius of curvature. Our calculations yields tensile-strain values for the top of the buckled structure ranging from ≈0.4% to ≈2%, that is, high enough to affect Si electronic properties significantly.[31]

We investigate scaling of the wrinkling instability with applied strain using a 55 nm-thick NM patterned in 20 μm wide ribbons and transferred to PDMS. The array of nanoribbons is then immersed in various solvents for 20 h. Each solvent produces a different swelling ratio, *S*, of the PDMS and hence different values of strain applied to the SiNM. We used N-methylpirrolidone ($\varepsilon = 0.9\%$), methanol ($\varepsilon = 1.5\%$), isopropyl alcohol ($\varepsilon = 3.7\%$), and acetone ($\varepsilon = 7.2\%$). The values of applied strain are calculated from the measured swelling ratio, *S*, of the PDMS in these solvents, as described in the Experimental Section. As shown by the profiles plotted in Figure 4e and the amplitude/length ratios in Figure 4f, the wrinkle length stays nearly constant while the amplitude increases with increasing strain. As a result, the radius of curvature at maximum amplitude decreases from ≈17 μm to ≈1 μm with increasing strain. We estimate corresponding values of tensile strain in the range of 0.1% to 1.2 % for the top (convex) surface of the wrinkled 55 nm SiNM.

3. Conclusions

We have presented a novel and facile approach for the fabrication of 2D and linear arrays of buckled structures on a compliant substrate. Our technology combines top-down tools (such as lithography and dry etching) with a self-assembly process, that is, deformation instabilities of thin films bonded to pre-strained elastomeric substrates. In our fabrication process

the substrates are strained by isotropic volume expansion in solvents, eliminating the need for any complex equipment[3,4] for straining the substrates and guaranteeing uniform applied strain over large areas. Furthermore with our approach linear arrays of both wrinkled and buckle-delaminated structures are obtained simply by varying the thickness of the NM. Currently used techniques to obtain ordered arrays of buckle-delaminated structures are based on creating film/substrate interfaces with different adhesion strengths via patterning and O_2 plasma treatment of selected PDMS surface regions prior to NM transfer.[4] In this case the weakly bonded portion of the film (i.e., the portion bonded to untreated PDMS areas) buckles, whereas the rest of the film remains flat on the substrate surface. Our process eliminates the need for this extra processing step and expands the range of film/substrate pairs that may be used.

We achieved a large degree of control on the out-of-plane and in-plane dimensions of the fabricated objects and we are able to pre-determine position and arrangement of buckled channels on the substrate surface. We showed that the out-of-plane dimensions of the 3D structures can be tuned by varying NM thickness, or applied strain to the NM/PDMS structure through the use of different solvents. We showed that the arrangement of buckled structures on the surface can be defined a priori by patterning the membrane in a particular fashion before transfer to the PDMS substrate (see Figure 5S in Supporting Information).

In principle a large NM including areas of various thicknesses and areas patterned in different fashions (e.g., in arrays of stripes and interconnected islands of various shapes) can be defined by using top-down techniques to process the NM while bonded to its original substrate. Transfer of the NM to a compliant substrate and subsequent treatment in solvent can be used to obtain 2D and linear arrays of buckles of different height or length or spacing on the same substrate and in a single processing step. After buckling-delamination has occurred on the compliant substrate in the steps described in this paper, the compliant substrate can be made resistant to subsequent influences of solvents by applying surface treatments or coating to avoid deformation of the substrate (and the buckled channels) during applications in fluidics or in further processing steps.[33]

Finally we highlight that our approach can be applied to a large variety of film/soft substrate combinations and chemical straining agents (in both liquid and vapor phase) offering a new research perspective and encouraging further development of a large variety of fields, ranging from flexible electronics and optoelectronics to chemical analysis, system biology, microfluidics, and optofluidics.

4. Experimental Section

Nanomembranes Fabrication and Transfer to the Compliant Host: Two-dimensional and linear arrays of buckled structures on PDMS were fabricated using SiNMs with thicknesses varying between minimum and maximum values of 17 and 270 nm. Silicon-on-insulator (SOI) wafers, consisting of a 150–270 nm-thick Si template, a 150–3000 nm-thick buried oxide (BOX) layer, and a bulk Si handle layer, were used as starting substrates. Thinner SiNMs were obtained from a given SOI samples by thermally oxidizing the starting Si templates and removing the SiO_2 grown on the surface in an HF (49% vol.) solution. The thickness of the NM was measured by X-ray diffraction or reflectometry. SiNMs were patterned in 20–100 μm wide stripes with a 20–100 μm pitch to fabricate linear arrays of buckle-delaminated/wrinkled structures, whereas buckled channel networks were obtained by patterning NMs in a checker-board fashion with holes of rectangular shape. The lateral dimensions of the SiNMs varied between 0.4 and 1 cm. Patterning of the Si templates before release was achieved by optical lithography and reactive ion etching with SF_6/O_2. SiNMs were released from the original substrate by selectively etching the BOX in the SOI wafer using HF (49% vol.). After complete removal of the BOX, two different techniques were used to transfer the released NMs to the new host, namely the elastomeric substrate. In one case the SiNMs were floated off in deionized (DI) water and here transferred onto the host. In another case the NMs were released, allowed to weakly bond back to the original substrate (i.e., the Si handle wafer) and subsequently peeled off using the elastomer substrate as a "stamp".

Fabrication and Characterization of the PDMS Substrate in Solvents: The PDMS substrate was prepared by casting a liquid PDMS mixture (10:1 weight ratio of silicone elastomer to curing agent, Sylgard 184, Dow Corning) onto a chemically cleaned Si wafer and curing for 4 h at 85 °C. The thickness of the PDMS substrate was approximately 3 mm. After 20 min of ultrasonication in DI water, the PDMS was dried and then exposed to oxygen plasma for 30 s with a power of 50 W.

Solvents were obtained from Sigma-Aldrich Co. (St. Louis, MO), Fisher Scientific Co. (Pittsburgh, PA), and VWR (Radnor, PA) and used as received.

Swelling ratios of PDMS in various solvents at room temperature were obtained by measuring the side-lengths of solid rectangular pieces of PDMS before and while being immersed in a solvent. We treated the PDMS pieces in each solvent for a time varying between 1.5 and 22 h at 25 °C. Under these conditions, swelling reached equilibrium (i.e., the dimensions of the PDMS solid did not change with time). Indeed we measured maximum swelling for the PDMS after ≈1 h treatment in solvents. The pieces were imaged while immersed in the solvent, using a CCD camera connected to a Wild 420 microscope. The side-lengths of the pieces were measured directly on the digitized image, using Nikon NIS-Elements software version 3.06 (Nikon Corp.). We measured the four side-lengths for three different rectangular pieces of PDMS for each solvent. To confirm uniformity of the elastomer swelling over an area larger than transferred NMs we used PDMS specimens with ≈1.2 cm × 1.4 cm lateral dimensions. All measured lengths were included in a relative error of 3%. Swelling ratios were calculated as $S = D_{sol}/ D_{air}$ where D_{sol} and D_{air} are the side-lengths of the PDMS specimens in solvent and in air, prior to treatment in solvent. The applied strain to the NM is calculated as $\varepsilon = \frac{D_{sol} - D_{air}}{D_{air}} = S - 1$.

Fabrication and Characterization of 2D and Linear Arrays of Buckled Structures: SiNMs are transferred to plasma treated PDMS substrates immediately after release. A time of ≈20 h elapses between transfer of the NM to the PDMS and treatment in solvent. We expect that any water trapped between the film and the substrate has diffused out of the interface over this time. Immersion in solvent is performed in glass beakers at room temperature. The duration of immersion varies between a minimum time of 30 min to a maximum time of 24 h. Controlled buckling of the NM is then achieved by exposing the sample to air at room temperature.

Amplitude and length of the wrinkled or buckle-delaminated structures were measured using three independent techniques, atomic force microscopy in tapping mode (using a MultiMode AFM (Digital Instrument-Veeco)), white-light interferometry (using a Zygo NewView 7200 optical interferometer), and scanning electron microscopy (using a Zeiss 1540XB Cross-beam Focused Ion Beam SEM).

Each data point in Figures 2b,4 is obtained as an average of amplitude versus corresponding length of 20 buckled structures randomly selected over NM areas ranging from 0.4 cm × 0.6 cm to 1 cm × 1 cm. The error bars in Figures 2b,4d–f include both the uncertainty of the three measurement techniques and the standard deviation of the 20 measured structures. The radii of curvature plotted in Figure 4d–f result

from averaging values measured for 20 structures at the maximum amplitude of the buckle.

Raman Spectroscopy of SiNMs: We performed Raman spectroscopy using a LabRAM Aramis (Horiba Jobin Yvon) Confocal Raman Microscope equipped with an excitation source operating at ≈633 nm. In our measurements the laser power was attenuated from 6 mW to ≈0.6 mW and focused to ≈2 µm using a 50× microscope objective lens.

Supporting Information

Supporting Information is available from the Wiley Online Library or from the author.

Acknowledgements

The work of F.C and M.G.L., as well as maintenance of the facilities used in this work, were supported by DOE, grant DE-FG02-03ER46028. The contributions of K.T. were supported by AFOSR. The authors thank Dr. D. S. Grierson and Dr. D. E. Savage for fruitful discussion.

Received: September 11, 2013
Published online: October 14, 2013

[1] D. S. Gray, J. Tien, C. S. Chen, *Adv. Mater.* **2004**, *16*, 393.
[2] S. P. Lacour, J. Jones, S. Wagner, T. Li, Z. Suo, *Proc. IEEE* **2005**, *93*, 1459.
[3] H. C. Ko, M. P. Stoykovich, J. Song, V. Malyarchuk, W. M. Choi, C.-J. Yu, J. B. Geddes, J. Xiao, S. Wang, Y. Huang, J. A. Rogers, *Nature* **2008**, *454*, 748.
[4] H. C. Ko, G. Shin, S. Wang, M. P. Stoykovich, J. W. Lee, D.-H. Kim, J. S. Ha, Y. Huang, K.-C. Hwang, J. A. Rogers, *Small* **2009**, *5*, 2703.
[5] N. Bowden, S. Brittain, A. G. Evans, J. W. Hutchinson, G. M. Whitesides, *Nature* **1998**, *393*, 146.
[6] T. Ohzono, S. I. Matsushita, M. Shimomura, *Soft Matter* **2005**, *1*, 227.
[7] H. Mei, R. Huang, J. Y. Chung, C. M. Stafford, H. H. Yu, *Appl. Phys. Lett.* **2007**, *90*, 151902.
[8] H. Mei, C. M. Landis, R. Huang, *Mech. Materials* **2011**, *43*, 627.
[9] A. Chen, D. K. Lieu, L. Freschauf, V. Lew, H. Sharma, J. Wang, D. Nguyen, I. Karakikes, R. J. Hajjar, A. Gopinathan, E. Botvinick, C. C. Fowlkes, R. A. Li, M. Khine, *Adv. Mater.* **2011**, *23*, 5785.
[10] T. Ohzono, H. Monobe, K. Shiokawa, M. Fujiwara, Y. Shimizu, *Soft Matter* **2009**, *5*, 4658.
[11] W. H. Koo, S. M. Jeong, F. Araoka, K. Ishikawa, S. Nishimura, T. Toyooka, H. Takezoe, *Nat. Photonics* **2010**, *4*, 222.
[12] D. Yuvaraj, M. B. Kadam, O. Shtempluck, E. B. Buks, *IEEE J. Microelectromech. Syst.* **2012**, *22*, 430.
[13] W. Song, D. Psaltis, *Lab Chip* **2013**, *13*, 2708.
[14] S. A. Scott, M. G. Lagally, *J. Phys. D: Appl. Phys.* **2007**, *40*, R75.
[15] F. Cavallo, M. G. Lagally, *Soft Matter* **2010**, *6*, 439.
[16] J. A. Rogers, M. G. Lagally, R. G. Nuzzo, *Nature* **2011**, *477*, 45.
[17] J. N. Lee, C. Park, G. M. Whitesides, *Anal. Chem.* **2003**, *75*, 6544.
[18] J. Song, H. Jiang, Z. J. Liu, D. Y. Khang, Y. Huang, J. A. Rogers, C. Lu, C. G. Koh, *Int. J. Solids Struct.* **2008**, *45*, 3107.
[19] E. Anastassakis, A. Pinczuk, E. Burstein, *Solid State Comm.* **1970**, *8*, 133.
[20] A. Ploessl, G. Kraeuter, *Mat. Sci. Eng. R* **1999**, *R25*, 1.
[21] G. S. Higashi, Y. J. Chabal, G. W. Trucks, K. Raghavachari, *Appl. Phys. Lett.* **1990**, *56*, 656.
[22] U. Goesele, Q. Y. Tong, *Ann. Rev. Mater. Sci.* **1998**, *28*, 215.
[23] X. Zhao, S. A. Scott, M. Huang, W. Peng, A. M. Kiefer, F. S. Flack, D. E. Savage, M. G. Lagally, *Nanoscale Res. Lett.* **2011**, *6*, 402.
[24] S. K. Sia, G. M. Whitesides, *Electrophoresis* **2003**, *24*, 3563.
[25] D. C. Duffy, J. C. McDonald, O. J. A. Schueller, G. M. Whitesides, *Anal. Chem.* **1998**, *70*, 4974.
[26] J. C. McDonald, D. C. Duffy, J. R. Anderson, D. T. Chiu, H. Wu, O. J. A. Schueller, G. M. Whitesides, *Electrophoresis* **2000**, *21*, 27.
[27] S. Timoshenko, *J. Opt. Soc. Am.* **1925**, *11*, 23.
[28] K. L. Johnson, *Contact Mechanics*, Cambridge University Press, UK **1987**.
[29] G. C. Sih, H. Liebowitz, in *Fracture, An Advanced Treatise*, Vol. *2*, p. 68, Academic Press, London, UK **1968**.
[30] H. H. Yu, J. W. Hutchinson, *Int. J. Fract.* **2002**, *113*, 39.
[31] K. Rim, J. Chi, H. Chen, K. A. Jenkins, T. Kanarsky, K. Lee, A. Mocuta, H. Zhu, R. Roy, J. Newbury, J. Ott, K. Petrarca, P. M. Mooney, D. Lacey, K. Koester, K. Chan, D. Boyd, M. Ieong, H.-S. Wong, *IEEE Symposium on VLSI Tech. Proc.* **2002**, *2002*, 98.
[32] J. R. Sánchez-Pérez, C. Boztug, F. Chen, F. F. Sudradjat, D. M. Paskiewicz, R. B. Jacobson, M. G. Lagally, R. Paiella, *Proc. Natl. Acad. Sci.* **2011**, *108*, 18893.
[33] J. Zhou, A. Vera-Ellis, N. H. Voelcker, *Electrophoresis* **2010**, *31*, 2.